



Reverse-engineering of biochemical reaction networks from spatio-temporal correlations of fluorescence fluctuations

Natsuki Tanaka^{a,b}, Garegin A. Papoian^{a,c,*}

^a Molecular and Cellular Biophysics Program, University of North Carolina, Chapel Hill, USA

^b Department of Biochemistry and Biophysics, University of North Carolina, Chapel Hill, USA

^c Department of Chemistry, University of North Carolina, Chapel Hill, USA

ARTICLE INFO

Article history:

Received 20 December 2009

Received in revised form

31 January 2010

Accepted 12 February 2010

Available online 18 February 2010

Keywords:

Spatially embedded signaling networks

Stochastic simulations

Simulated annealing

FRET biosensor

ABSTRACT

Recent developments of fluorescence labeling and highly advanced microscopy techniques have enabled observations of activities of biosignaling molecules in living cells. The high spatial and temporal resolutions of these video microscopy experiments allow detection of fluorescence fluctuations at the timescales approaching those of enzymatic reactions. Such fluorescence fluctuation patterns may contain information about the complex reaction–diffusion system driving the dynamics of the labeled molecule. Here, we have developed a method of identifying the reaction–diffusion system of fluorescently labeled signaling molecules in the cell, by combining spatio-temporal correlation function analysis of fluctuating fluorescent patterns, stochastic reaction–diffusion simulations, and an iterative system identification technique using a simulated annealing algorithm. In this report, we discuss the validity and usability of spatio-temporal correlation functions in characterizing the reaction–diffusion dynamics of biomolecules, and demonstrate application of our reaction–diffusion system identification method to a simple conceptual model for small GTPase activation.

© 2010 Elsevier Ltd. All rights reserved.

1. Introduction

Cell signaling networks control a wide range of physiological processes, including development, immunological response, programmed cell death, and cancer transformation. However, it is often difficult to uncover protein interactions behind many biochemical signaling networks and elucidate the corresponding kinetic mechanisms. With recent technological advances, several systems biological approaches have been suggested to tackle this problem, including such techniques as flow cytometry (Chen et al., 2008), RNA interference (Bakal et al., 2008), high-throughput mass spectroscopy (Yu et al., 2008) and other biochemical methods (Janes et al., 2005; Barrios-Rodiles et al., 2005).

In most of these methods, however, data are collected not at a single cell level but from a population of cells (i.e. unresolved spatially), at a low temporal resolution, where the experiment lasts for minutes to hours. On the other hand, the individual kinetic rates of biosignaling networks are often in a sub-second range or faster, since the elementary processes of intracellular signaling typically involve either diffusion-limited association or fast enzymatic reactions. Furthermore, increasing evidences

points to the importance of noise in signal transduction processes, which, in turn, manifests itself in cell-to-cell variability of signal response within a mono-clonal cell population (Cai et al., 2006; Chang et al., 2008; Choi et al., 2008). Theoretical studies also predict that a variety of consequences may emerge as a result of noisy signaling (Kaern et al., 2005; Monine and Haugh, 2005; Walczak et al., 2005; Lu et al., 2007; Artyomov et al., 2007; Locasale et al., 2007; Acar et al., 2008), including stochastic resonance (Lan and Papoian, 2007a) and strongly nonlinear effects (Lan and Papoian, 2007b, 2006a; Lan et al., 2006).

Most of recent research on biological noise focused on studying gene expression dynamics (Mettetal et al., 2006). In such systems, the noise is almost always regarded as spatially homogeneous: kinetics of transcription and translation (the latter including a step by step synthesis of a protein) in gene expression dynamics is slow enough that relatively fast diffusion renders the cell well-stirred. Since it has been shown that stochastic chemical kinetics can be exactly expressed in the language of quantum field theory (QFT) (Mattis and Glasser, 1998; Walczak et al., 2005; Lan et al., 2006), a well-stirred process would correspond to a zero-dimensional (0D) QFT problem. On the other hand, cell signaling kinetics, as found in cell motility regulation and chemotactic sensing, is usually fast, based on enzymatically driven reactions of phosphorylation, ATP or GTP hydrolysis, and also protein binding, where the latter kinetics is often diffusion limited. Therefore, spatial heterogeneity cannot be ignored in cellular information processing by biochemical signaling networks. When accompanied by noise,

* Corresponding author at: Department of Chemistry, University of North Carolina, Chapel Hill, USA. Tel.: +1 919 962 8037; fax: +1 919 962 2388.
E-mail address: gpapoian@unc.edu (G.A. Papoian).

these processes may be considered equivalent to 3D QFT, difficult to solve either analytically or numerically (Mattis and Glasser, 1998; Lan and Papoian, 2008), compared to the 0D case. Thus, in order to fully characterize spatially heterogeneous fluctuations in rapid biosignaling networks, very high resolution measurements and appropriate analysis methods are of great importance, significantly different from tools used to study well-mixed chemical reaction networks, in particular gene expression dynamics (Dunlop et al., 2008; Cox et al., 2008; Warmflash and Dinner, 2008).

Fluorescence video microscopy experiments address some of these challenges by allowing one to observe individual living cells with high spatial resolution, where the diffraction limit of visible light is few hundred nanometers, and at high temporal resolution, with video frame rates up to ~ 33 ms (Petty, 2007; Inoué and Spring, 1997). Thus, the temporal resolution limit of the fluorescence video microscopy is close to the timescales of many enzymatic reactions (Zhang et al., 2004). Furthermore, microscopy has another unique advantage that it can observe the fluorescently labeled molecules in the cell simultaneously with the cell's morphological changes. Such unique advantages of microscopy are perhaps best illustrated in the study of molecular motors, in which the individual steps (on the order of nanometers) of single motor proteins are directly observed (at a sub-second temporal resolution) (Sakamoto et al., 2008). These measurements, as well as others using such techniques as laser tweezers and piezoelectric nano-actuators (Svoboda et al., 1994; Kojima et al., 1997), have shed light on the highly fluctuating nature of molecular motor steps because of an intrinsically noisy microscopic environment. This important aspect in the work of biological nano-machines is also being thoroughly examined theoretically and computationally, including a spatially resolved master equation approach (Das and Kolomeisky, 2008) and a consideration based on the fluctuation-dissipation theorem (Harada and Sasa, 2007). Furthermore, fluorescent biomarkers have remarkably advanced in the last decade (Giepmans et al., 2006). Especially, Förster resonance energy transfer (FRET, Förster, 1959) probes enable experimentalists to monitor essential activities of signaling proteins, such as conformational changes and binding to their substrates. Many FRET biosensors for key biosignaling molecules have been developed so far, including heterotrimeric G-proteins (Janetopoulos et al., 2001; Bünemann et al., 2003), small GTPases (Pertz et al., 2006; Kraynov et al., 2000; Nalbant et al., 2004; Mochizuki et al., 2001), kinases/phosphatases (Lu et al., 2008; Zhang et al., 2001; Sasaki et al., 2003; Violin et al., 2003), and other important signaling enzymes and small molecules, such as PLC, PIPs, Ca^{2+} and cAMP (van der Wal et al., 2001; Parent et al., 1998; Miyawaki et al., 1997; Adams et al., 1991). Thus, nowadays, many key signaling processes in the cell may be monitored via specially designed fluorescent biosensors.

The combination of fluorescence video microscopy with newly developed FRET biosensors allows to capture fluctuating spatio-temporal fluorescence patterns, which, in turn, encode information about the underlying microscopic signaling dynamics. Diffusion of molecules in a cell results in specific spatial fluctuations at the microscopic scale. Also, since enzymes work stochastically at the single molecular levels (Lu et al., 1998), the interconversion between FRET and non-FRET states also produces fluctuations at the enzymatic reaction timescales. Thus, the biosignaling processes at these time and length scales may be regarded as a stochastic reaction-diffusion (RD) system. If indeed the observed fluorescence fluctuations reflect the structure and dynamics of this RD system (Petrášek and Schwille, 2008), it may be possible to extract (reverse-engineer) some architectural links and all kinetic rates of the underlying signaling network. Thus, how to analyze the observed fluorescence fluctuation patterns to

identify the corresponding RD system is a problem of great practical importance.

Correlation functions are effective for analyzing noisy fluctuations. For example, in fluorescence correlation spectroscopy (FCS), one analyzes the temporal correlation function of the observed fluorescence fluctuations. FCS has been successfully applied to investigate biomolecules in living cells, allowing to obtain such information as diffusion coefficients (Wawrezynieck et al., 2005) and chemical reaction rates (Hegener et al., 2004). Similarly, a correlation analysis can be applied to video microscopy data. Although video recording does not achieve as good a time resolution as FCS does (Burkhardt and Schwille, 2006), video data have an advantage that they contain spatial information in addition to the time-series information, allowing one to perform a spatio-temporal correlation analysis. Wiseman and colleagues have developed spatio-temporal image correlation spectroscopy (STICS) (Hebert et al., 2005) and k-space image correlation spectroscopy (kICS) (Kolin et al., 2006) to analyze the dynamics of fluorescent particles on the cell membranes. They showed that the spatio-temporal correlation analyses are advantageous over FCS in that the fluctuations due to diffusion and due to reactions are clearly distinguishable, because they appear distinctively in the spatial and temporal correlation functions. This made it possible to analyze RD systems with nonexponential decay, such as the blinking dynamics of quantum dots (Bachir et al., 2008).

Although most of the previous spatio-temporal correlation analyses were performed on video microscopy images of fluorescent particles or speckles in which individual motions of the molecules are recognizable, this analysis method may also be applied to continuous fluorescence images in which individual fluorescent particles are not resolved, including video microscopy data obtained by *in vivo* FRET-biosensor imaging (as illustrated in Fig. 6), as long as the fluorescence fluctuations are detectable. The fluctuations in such FRET imaging may contain valuable information on the dynamics and mechanisms of biosignaling, since the high-FRET and low-FRET states of FRET biosensors represent the active/inactive states of the probed proteins or indicate the binding/unbinding of their binding partners. In the previous works, the fluorescence fluctuations were analyzed for relatively simple reactions by fitting their correlation functions to theoretical curves. However, this approach becomes intractable if the RD system is non-trivial or not fully characterized.

In this work, we have devised a RD system identification approach as an alternative to the theoretical fitting described above. In this approach, the spatio-temporal fluctuation patterns of biosignaling RD systems are simulated using our in-house stochastic RD simulation software, and the obtained patterns are quantitatively characterized using spatio-temporal correlation functions (STCFs). To find the best computational model that can reproduce the experimentally observed spatio-temporal FRET signal fluctuation patterns, we used an iterative optimization technique, based on the simulated annealing (SA) algorithm (Kirkpatrick et al., 1983; Erban et al., 2007), allowing us to obtain the model parameter values for complicated RD models, which could not be treated analytically. We are not aware of any prior technique, neither analytical nor numerical, where spatial correlations may be used in addition to temporal correlations to extract kinetic parameters in an arbitrary chemical reaction network.

2. Methods

2.1. Stochastic reaction-diffusion simulations

A two-dimensional stochastic RD simulator was implemented (Fig. 1) to perform RD simulations that take into account the

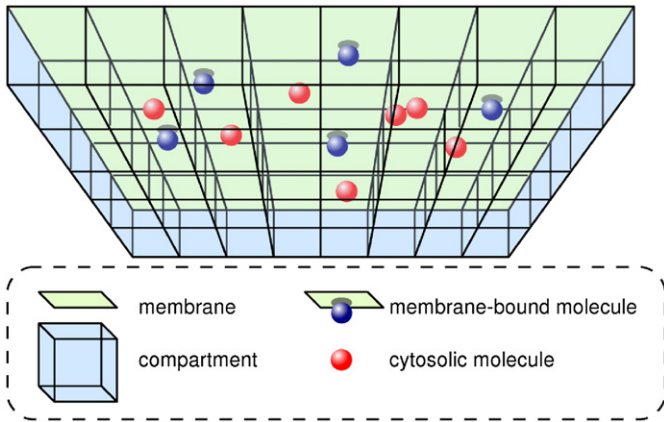


Fig. 1. A conceptual drawing of the geometric scheme for our stochastic reaction-diffusion simulation program is shown. The two-dimensional square geometry is composed of small boxes. The ceiling of the box is the cell membrane. The small GTPases may attach to the membrane or detach.

discreteness in the particle number fluctuations (the fluctuations in the number of molecules due to reactions and diffusion). These fluctuations are fundamentally present in chemically reacting systems, and play a major role when there are only a few molecules present in the reacting volume, which is a common scenario in cell signaling. Our simulation program solves a spatially embedded chemical master equation (SECME) (Isaacson, 2008; Lan and Papoian, 2008; Zhuravlev and Papoian, 2009), using the Gillespie (1977) algorithm. The original Gillespie algorithm does not take diffusion into consideration, since the algorithm assumes that chemical reactions take place in a very small volume in which diffusion of the molecules can be ignored (thus, the molecules are assumed to be well-mixed). In our implementation, a separate Gillespie simulator is used within each “voxel” with the side $l = 1 \mu\text{m}$, and diffusion of molecules is represented by stochastic “hopping” of molecules from one voxel to the adjacent one, with the rate τ_D^{-1} . τ_D is the characteristic diffusion time of the molecule, which is related to the diffusion coefficient D by $D = l^2 \tau_D^{-1}$ (van Kampen, 1992).

The reaction-diffusion system is placed in a 2D lattice of size $n \times m$. In this study, a square lattice 20×20 was used, which correspond to a $20 \times 20 \mu\text{m}^2$ slab. The distribution pattern of a molecular species A in this 2D slab geometry can be described by an $n \times m$ matrix \mathbf{A} . A matrix element $A_{ij} \in \mathbb{N}$ represents the number of molecules at the voxel at (i, j) . Let us define a matrix $\mathbf{1}_{ij}$, having zeroes everywhere except for the matrix element at ij (the corresponding element being 1), such that $\mathbf{A} + \mathbf{1}_{ij}$ denotes an increment of a molecule A in the voxel at (i, j) , and $\mathbf{A} - \mathbf{1}_{ij}$ denotes the corresponding decrement (reminiscent of the action of ladder operators in quantum mechanics).

2.1.1. Rho small GTPase reaction-diffusion model

In what follows below, we show the SECME for our small GTPase Rho reaction-diffusion model (Fig. 2). A Rho molecule may exist either in a membrane-bound or cytosolic state since this small GTPase has a lipid post-translational modification (Lu et al., 1998). On the other hand, the activation and inactivation of Rho are simplified to be first-order reversible forward and backward reactions, although these processes in reality may be controlled by many regulator molecules (Jaffe and Hall, 2005).

Let $P(\mathbf{m}, \mathbf{m}^*, \mathbf{c}, \mathbf{c}^*, t)$, denote the probability that the Rho molecules in the four different states are distributed in the 2D geometry in a particular pattern as described by $\mathbf{m}, \mathbf{m}^*, \mathbf{c}, \mathbf{c}^*$ at time t . Here m_{ij} denotes the number of membrane bound Rho at 2D lattice site ij , c_{ij} denotes the number of cytosolic Rho at 2D

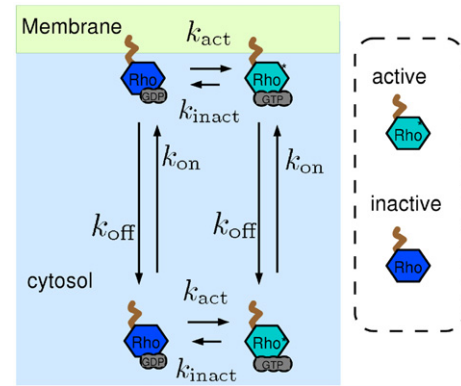


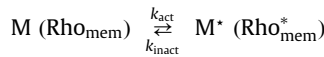
Fig. 2. The Rho small GTPase reaction-diffusion model that we used in our stochastic reaction-diffusion simulations is conceptually sketched. See Table 1 for the parameter values.

lattice site ij , and star superscripts indicate the corresponding activated forms. Then P obeys the following SECME:

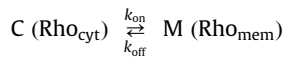
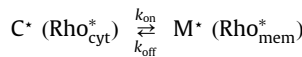
$$\frac{dP}{dt} = (\hat{M} + \hat{D})P \quad (1)$$

where \hat{M} and \hat{D} are the reaction and diffusion operators, respectively.

The reaction equations for our Rho model are the activation/inactivation processes,



and the association/dissociation reactions to the inner leaflet of the cytoplasmic membrane,



For example, the first out of eight, chemical reactions above (i.e. activation of membrane bound Rho) becomes translated into the following reaction term in the SECME:

$$\hat{M}_{M \rightarrow M^*} P = \sum_{i=1}^n \sum_{j=1}^m (-k_{\text{act}} m_{ij} P(\mathbf{m}, \mathbf{m}^*, \mathbf{c}, \mathbf{c}^*, t) + k_{\text{act}} (m_{ij} + 1) P(\mathbf{m} + \mathbf{1}_{ij}, \mathbf{m}^* - \mathbf{1}_{ij}, \mathbf{c}, \mathbf{c}^*, t)) \quad (2)$$

Analogous equations are written for the remaining seven chemical reactions. The diffusion term for membrane bound inactivated Rho (i.e. species M), reads,

$$\hat{D}_M P = \tau_{\text{Dmem}}^{-1} \sum_{i=1}^n \sum_{j=1}^m \sum_{k=1}^n \sum_{l=1}^m L_{ijkl} (-m_{ij} P(\mathbf{m}, \mathbf{m}^*, \mathbf{c}, \mathbf{c}^*, t) + (m_{kl} + 1) P(\mathbf{m} + \mathbf{1}_{kl} - \mathbf{1}_{ij}, \mathbf{m}^*, \mathbf{c}, \mathbf{c}^*, t)) \quad (3)$$

where τ_{Dmem} and τ_{Dcyt} are the characteristic diffusion times for the membrane-bound and cytosolic Rho molecules, respectively, and L_{ijkl} a member of the set $\mathbf{L} = \{L_{ijkl} | i, k \in \{1 \dots n\}, j, l \in \{1 \dots m\}\}$, which represents the connectivity of the 2D lattice geometry: If the voxels at (i, j) and at (k, l) are “connected” ($L_{ijkl} = 1$), a molecule can “diffuse” from the voxel at (i, j) to the voxel at (k, l) and vice versa. If the voxels are “not connected” ($L_{ijkl} = 0$), “diffusion” is not allowed between these voxels. \mathbf{L} in our model is chosen such that the molecules can diffuse from the current voxel to the adjacent

voxels, up, down, left or right, but not diagonally. In addition to membrane bound Rho, three analogous diffusional terms are written for cytosolic Rho (species C with diffusion constant $\tau_{D_{\text{cyt}}}$), and two activated forms of Rho (C^* with $\tau_{D_{\text{cyt}}}$ and M^* with $\tau_{D_{\text{mem}}}$).

This Rho small GTPase system is a simplistic model for recent experimental observations which used FRET-based biosensors in living cells (Pertz et al., 2006; Nalbant et al., 2004; Kraynov et al., 2000).

2.1.2. Diffusion-only system

We have also performed two sets of simple simulations to examine the way the number fluctuations caused by reactions only are distinguishable from fluctuations in a diffusion only system, when the corresponding spatio-temporal correlation functions are compared. The RDME for a molecule A that does nothing but diffuse is the following:

$$\frac{d}{dt}P(\mathbf{C}^A, t) = \sum_{i=1}^n \sum_{j=1}^m \sum_{k=1}^n \sum_{l=1}^m \tau_D^{-1} L_{ijkl} P(\mathbf{C}^A - 1_{ij} + 1_{kl}, t) \quad (4)$$

2.1.3. Reaction-only system

In the reaction-only system, a fluorescent molecule F converts back and forth to a temporal non-fluorescent state X,



The RDME for this system is

$$\begin{aligned} \frac{d}{dt}P(\mathbf{C}^F, \mathbf{C}^X, t) = & \sum_{i=1}^n \sum_{j=1}^m \left([k_f C_{ij}^F P(\mathbf{C}^F + 1_{ij}, \mathbf{C}^X - 1_{ij}, t)] \right. \\ & \left. + [k_b C_{ij}^X P(\mathbf{C}^F - 1_{ij}, \mathbf{C}^X + 1_{ij}, t)] \right) \end{aligned} \quad (6)$$

This system resembles an experiment performed by Dickson et al. (1997), where GFP molecules are congealed in a gel and their blinking was observed by video microscopy.

2.2. Spatio-temporal correlation function (STCF)

A spatio-temporal correlation function is computed from the spatially and temporally resolved concentration profile of some molecular species. A fluorescence intensity recorded by video microscopy is proportional to the concentration of the labeled molecule (Elson and Madge, 1974). Let $I(\vec{R}, t)$ be the fluorescence intensity at position $\vec{R} = (x, y)$ at time t . The spatio-temporal correlation at distance $\vec{r} = (\xi, \eta)$ and time lag τ is defined as

$$STCF(r, \tau) = \frac{\langle \delta I(\vec{R}, t) \cdot \delta I(\vec{R} + \vec{r}, t + \tau) \rangle}{\langle I(\vec{R}, t) \rangle \langle I(\vec{R}, t + \tau) \rangle} \quad (7)$$

where $\delta I(\vec{R}, t)$ is the fluorescence fluctuation, $\delta I(\vec{R}, t) = I(\vec{R}, t) - \langle I(\vec{R}, t) \rangle$. The STCF may be defined as $STCF(\xi, \eta, \tau)$ as in Kolin and Wiseman (2007), in which case the dynamics difference between x and y directions may be characterized, enabling to detect, for example, an existence of a directed transport of molecules. If the system is spatially isotropic, the distance $r = |\vec{r}| = \sqrt{\xi^2 + \eta^2}$ may be used instead.

2.3. SA-based RD system identification

If the biochemical reaction network is known, but the rate constants have not been determined, one can vary the latter values to obtain the best fits to the STCF curves. In cases, when small uncertainty may exist in the network connections, one could fit the experimental data with alternative models, that, in

turn, may help to choose the most optimal network architecture. We have devised an iterative computational simulation approach to tackle these problems. With the stochastic simulation program, fluctuation patterns of RD systems can be computed for arbitrary RD models. By iteratively optimizing the difference between the computationally obtained fluctuation patterns with the data from an “unknown” system, one may be able to identify the best model for the observed system and quantitatively characterize the dynamics of this system.

However, since fluctuations are stochastic in nature, the spatio-temporal fluctuation patterns of RD systems cannot be directly compared (i.e., two separate observations of an identical RD system would give different fluctuation patterns). The STCF approach characterizes well such systems, because correlation functions describe the statistical properties of the fluctuation patterns. Therefore, by quantitatively comparing the STCF computationally obtained from a “trial” model with the “target” STCF from an unknown system, and by iteratively modifying the trial model to minimize the difference between the two STCFs, one may be able to identify the RD model for the system of interest. In this paper, we have developed a RD system identification method using the residual sum of squares (RSS) as the quantitative measure and the SA algorithm for the iterative optimization.

The STCFs were quantitatively compared by evaluating the RSS,
$$RSS = \sum_r \sum_\tau [STCF_1(r, \tau) - STCF_2(r, \tau)]^2. \quad (8)$$

The RSS is zero when $STCF_1(r, \tau)$ and $STCF_2(r, \tau)$ are identical, and is greater than zero if the two are different.

The SA technique (Kirkpatrick et al., 1983) is used to minimize this RSS. The technique is a Monte Carlo method to search a parameter space, which uses formal “temperature” and the Metropolis criterion to accept or reject newly found parameter sets during the course of optimization in order to avoid being trapped by local minima and reach the global minimum. This is achieved by occasionally accepting uphill moves on the “RSS landscape” while downhill moves are always accepted.

The iterative optimization process was implemented as follows: Firstly, the upper and lower bounds of the search ranges are defined for each parameter to be optimized. The narrower the parameter range, the more efficient the search process is. The program explores N -dimensional parameter space (N is the number of parameters to be optimized) by N -dimensional Brownian motion, which is initialized at a random location in the parameter space. Within a single iteration, a stochastic RD simulation is run at the current location of the search, and the resulting STCF is compared with the target STCF to obtain the RSS. This RSS value is subjected to the Metropolis criterion. This procedure is iteratively repeated, and the “temperature” is decreased during the course of iterations according to a preprogrammed schedule. In this program, the first 10% of the total steps is run with infinite temperature, meaning every step is unconditionally accepted. Then the temperature is determined based on the square root of variance found from the first 10% of the run. Temperature is linearly decreased as the iteration proceeds, and reaches zero when the 90% of the total steps is reached. The last 10% of the annealing is run with zero-temperature, meaning only downhill moves are accepted. The diffusion coefficient for N -dimensional Brownian motion is empirically chosen to be just large enough to explore the whole range of the parameter space. This diffusion coefficient was also linearly decreased to a fraction of the original at the end, effectively narrowing the parameter search space at the later stage of optimization, thus increasing search efficiency.

3. Results and discussion

3.1. Simple RD systems may be distinguished by their spatio-temporal correlation signatures

The STCFs show distinctive signatures of whether the number fluctuations are due to diffusion or chemical reactions. In Fig. 3, panels A–C show the STCFs of the diffusion-only systems, and the panels D–F show the reaction-only systems. The xz -plane intercept of a STCF represents the purely temporal correlation (autocorrelation) and yz -plane intercept is the purely spatial correlation.

The most prominent difference between the obtained STCFs of the reaction-only simulations and the diffusion-only simulations is seen in the spatial correlation part (along the r axis): There is no spatial correlation in the reaction-only systems, whereas there are some nonzero values at $r \geq 0$ in the diffusion-only cases. This is because the molecules in the reaction-only simulations do not diffuse at all, and their stochastic blinking reactions are completely independent from other molecules. On the other hand, diffusion-only simulation results show some positive spatial correlations at $r \geq 0$. This trend is most prominent at the fastest diffusion constant result (Fig. 3 F), and not recognizable at the lowest diffusion constant result (Fig. 3 D). The two sets of simulations (reaction-only and diffusion-only ones) illustrate that spatial correlations are primarily driven by diffusion.

The temporal part of the correlation functions becomes longer ranged as the parameter values become smaller, be it either the diffusion coefficient or the reaction rate constant. On the other hand, the purely spatial part of the correlation functions becomes shorter ranged as the diffusion coefficient decreases, and it vanishes in the reaction-only simulation results, where the diffusion coefficient of the molecule is zero.

When the blinking rate k_f , k_b is set greater than 1 s^{-1} , the resulting STCF becomes δ function-like, i.e., $STCF(r, \tau) \sim 0$ at other than $(r, \tau) = 0$ (data not shown), as binning was performed when computing the STCFs with the bin size of 1 s. Because of this, the temporal resolution limit of the STCFs shown in Fig. 3 is 1 s. (One can see that in Fig. 3 C where the rate is 1 s^{-1} , the STCF is already close to δ function-like.) Since these STCFs in Fig. 3 are calculated from simulation trajectories, the resolution can be improved to an arbitrary level if needed be, by narrowing the bin size. However, if a STCF is calculated from an experimental data, the time resolution of the experimental data sets the resolution limit of the STCF, which is $\sim 33 \text{ ms}$ for a typical CCD camera.

For these diffusion-only and reaction-only systems, analytically exact autocorrelation functions are known, which are a Lorentzian for the diffusion-only system (Elson and Madge, 1974), and an exponential decay for this simple reaction-only system (Starr and Thompson, 2001). While our stochastic simulation results agree qualitatively with these analytical predictions, the least-square fitting of theoretical curves and the correlation curves from our simulation results were not in good quantitative agreement (data not shown). This is because our stochastic simulation model uses strongly discretized spatial geometry, while the theories work with continuous space. However, the same problem occurs for experimentally observed fluorescence fluctuations using CCD camera and a fluorescence microscope, where the spatial and temporal resolution values are similar to those in our simulations. Generally, diffusion or reaction-kinetic parameters obtained by CCD-camera-based measurements are not as precise as those obtained by FCS measurements with much higher time resolution and smaller observation volume, where the latter are more straightforward to compare with analytical predictions. Still, even taking into account the current resolution limits, we found that results reported in this work provide useful information in interpreting and predicting the underlying RD systems, as elaborated below.

3.2. “Mutating” the Rho reaction network is clearly reflected in STCFs

Next, we have examined a simple RD model of a signaling molecule Rho (Fig. 2) to examine an RD system in which the molecules undergo both chemical reactions and diffusion. Rho is a small GTPase that plays a major role in regulating cell motility driven by the actin cytoskeletal processes. Its dynamics has been observed recently using a FRET biosensor (Pertz et al., 2006). One of the goals of our calculations was to gauge the change in STCFs as the wild-type model is perturbed in various ways. Fig. 4 shows the results of the simulations for the WT, CA and CS model. The STCFs were computed for the high-FRET states H . For all the simulations, all Rho molecules were prepared in the inactive, membrane-bound state at $t=0$.

In the CA simulation result, the time-lapse images turned greener in color as time progresses, indicating the equilibrium shifted toward the activated Rho states (Fig. 4, Time-Lapse Images). The STCFs for the CA and WT showed a distinctive difference: The temporal correlation decay of the STCF is milder

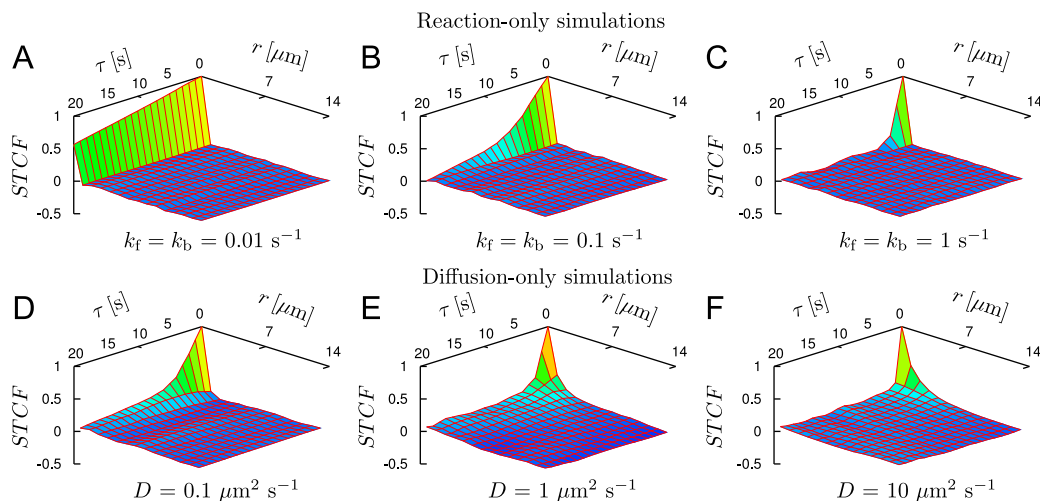


Fig. 3. Plots of STCFs from stochastic reaction–diffusion simulations are shown. The STCFs are computed for the concentration of the fluorescent species $[F]$. (A–C) The STCFs of simple 1st-order reversible reaction simulation results. (D–F) The STCFs of simple diffusion simulation results. The STCFs are normalized to 1 at the origin.

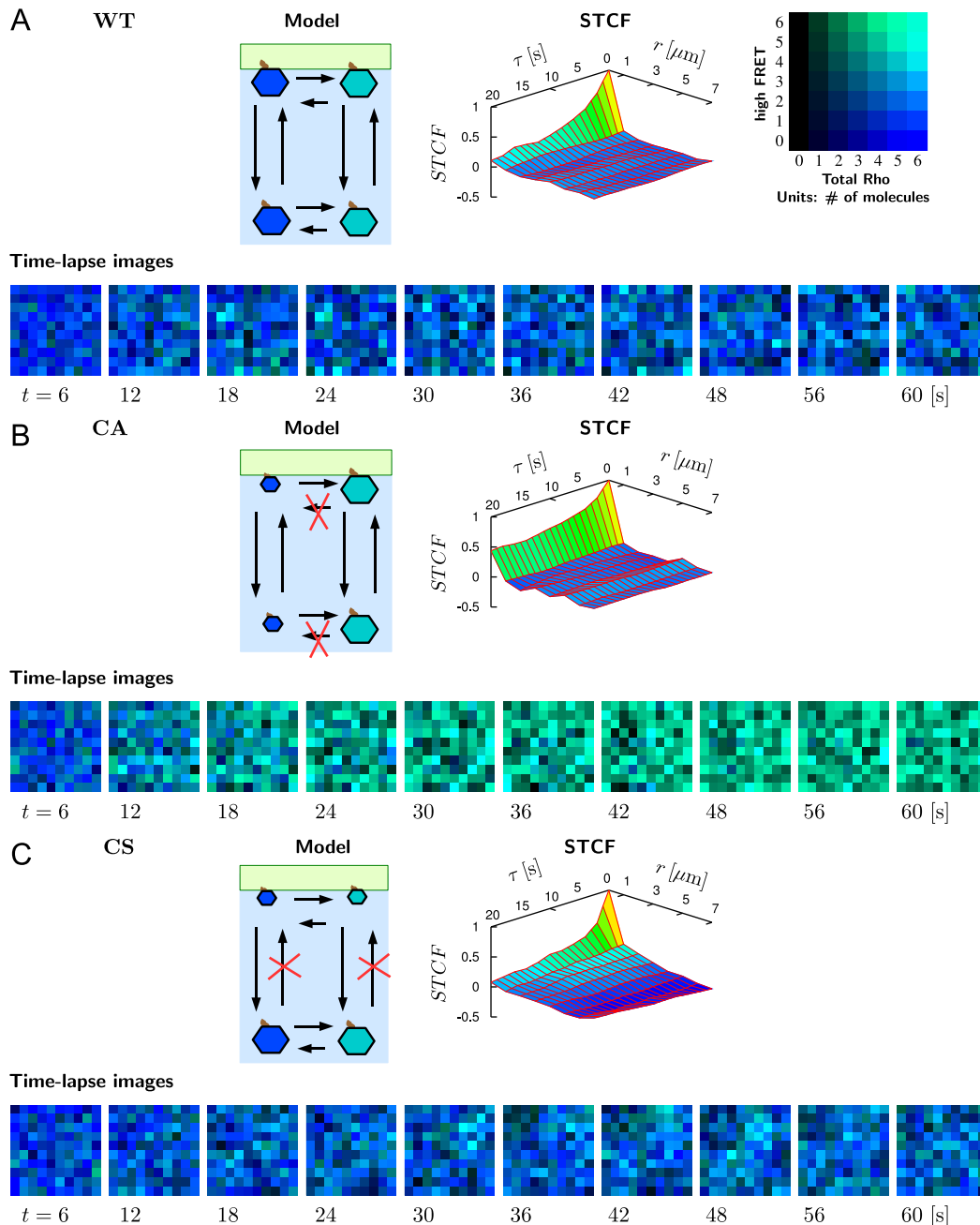


Fig. 4. The Rho small GTPase simulation results. The red crosses in the *model* cartoons indicate the inhibited transitions in the small GTPase model shown in Fig. 2. Each STCF was computed for the high-FRET states (*H*, see text) of the simulation result. The *time-lapse images* in each simulation show the temporal development of the simulation with 2-s intervals. The 20×20 lattice geometry corresponds to $20 \mu\text{m} \times 20 \mu\text{m}$. The total Rho ($H+L$) are shown in blue, the high-FRET states (*H*) are shown in green. The inset shows the color code table for the time-lapse images. (For interpretation of the references to color in this figure legend, the reader is referred to the web version of this article.)

than the other two STCFs for the WT and CS models. This is consistent with the fact that only in this model the turnover rate (k_f+k_b , i.e., one cycle of conversion from inactive to active back to inactive) is diminished. In the CS simulation result, the spatio-temporal fluctuation patterns were apparently not very different from the WT result (Fig. 4 A,C Time-lapse Images). However, the STCFs for the two simulation results were notably different: The STCF for the CS result showed a much higher spatial correlation than that of the WT result.

In summary, these simulations indicate that the spatio-temporal correlation analysis is effective in characterizing RD systems with coupled reactions and diffusion. A simple Rho GTPase activation model was used to examine the STCF of the

fluctuation patterns. Despite the minimalist design of the model, the system contained an internal degree of freedom (namely, cytosolic/membrane-bound states) that is not directly probed by the experimental observables (the high- and low-FRET states). The changes in the fluctuation dynamics were distinctively characterized upon some perturbations to the model. When the inactivation of Rho is inhibited in the CA model, the temporal correlation of the fluctuating pattern has increased, reflecting the slow turnover dynamics. This was also evident from the equilibrium shift toward high-FRET states (Fig. 4 B). In the CS model result, the effect of the arrest of Rho molecules in the cytosol was not readily recognizable from the video images, but was clearly noticeable in the STCFs. Thus, noisy fluctuation

Table 1

The parameter values and the search ranges used in the RD simulations and in SA based parameter optimization are listed.

Parameters	Wildtype (WT)	Constitutively active (CA)	Cytosolic sequestration (CS)	Search range in system identification
$k_{\text{inact}} \text{ (s}^{-1}\text{)}$	0.1	0.001	0.1	0.0005–0.2
$k_{\text{act}} \text{ (s}^{-1}\text{)}$	0.1	0.1	0.1	Fixed
$k_{\text{on}} \text{ (s}^{-1}\text{)}$	0.04	0.04	0.0004	0.0001–0.05
$k_{\text{off}} \text{ (s}^{-1}\text{)}$	0.04	0.04	0.04	Fixed
$D_{\text{cyt}} \text{ (}\mu\text{m}^2 \text{ s}^{-1}\text{)}$	0.5	0.5	0.5	Fixed
$D_{\text{mem}} \text{ (}\mu\text{m}^2 \text{ s}^{-1}\text{)}$	0.001	0.001	0.001	Fixed

Table 2

The reverse-engineering results for the WT model are shown.

WT (RSS=0.00330)	Original	Identified	Error	Error-interval ratio ^a (%)
$k_{\text{inact}} \text{ (s}^{-1}\text{)}$	0.100	0.0929	−0.0071	−3.6
$k_{\text{on}} \text{ (s}^{-1}\text{)}$	0.0400	0.0407	+0.0007	+1.4

^a The *error-interval ratio* values were calculated by the formula $\text{error}/[(\text{upper bound of the search range}) - (\text{lower bound of the search range})]$. The denominator (the interval) is 0.1995 for k_{inact} and 0.0500 for k_{on} . The parameter values for the search ranges are listed in Table 1.

patterns may contain useful information although they may not be directly recognizable, and the STCF is an effective way to reveal that information.

3.3. Kinetic parameters of the Rho reaction network were reverse-engineered from the STCFs

In the above Rho small GTPase simulations, it was found that the fluctuating dynamics of RD systems with coupled reactions and diffusion may be differentially characterized using STCFs. Therefore, we asked the next question of whether the parameters in the RD systems is identifiable by analyzing just their fluctuation patterns (or the STCFs derived thereof). For this purpose, we used the SA-based RD system identification method developed in this study. In this present paper, we report the identification of two parameters in the above small GTPase models, namely, k_{inact} and k_{on} out of the six parameters in the model (see Table 1 and Fig. 2). These two parameters are the ones that are varied in the CA and CS models relative to the WT model. The STCFs shown in Fig. 4 are used as the target STCFs. The values for parameters other than two parameters to be optimized and the overall framework of the RD system as shown in Fig. 2 were known to us beforehand.

Firstly, the WT model parameters were reverse-engineered. The parameter search ranges were chosen so that the kinetic parameter values for both the WT and the mutated models are covered, spanning nearly 3 orders of magnitude for k_{inact} and 2 orders of magnitude for k_{on} , as listed in Table 1. The reverse-engineered parameter values were in good agreement with the original values (see Table 2): The magnitude of error were −0.0071, or 0.71%, for k_{inact} and +0.0007, or 1.8% for k_{on} . Fig. 5 shows the locations of the identified parameter set in the 2D parameter space, as well as the RSS landscape that has been rendered as a result of the SA search process. The reverse-engineered parameter set is located in the same basin as the original parameter set.

To evaluate the effectiveness of the SA algorithm, we have introduced a quantitative measure, namely the error-interval ratio. This is the ratio between the absolute error and the size of parameter search range, or interval. When the interval is set wider, it becomes more difficult for the optimization becomes to reach the true value, if the number of iterations for the search is

held constant. This error-interval ratio serves as a kind of cost-performance indicator for our optimization results: In our single SA optimization process, 1600 iterations were performed, that is, 1600 different points in our 2D parameter space were explored, therefore, if the parameter space was evenly scanned on the 1600 grid points on the 40×40 lattice, the optimization would achieve a 2.5% (1/40) margin of error per parameter. However, the parameter value optimization in this STCF-based reverse-engineering is a more complicated task, because of the intrinsically noisy nature of fluctuations. Since the STCF is a statistical average quantity of stochastic fluctuations, the STCFs computed in this study bear margin of errors. The RSS, which is used as an evaluation criteria in SA optimization, inherits these statistical errors. Since the RSS value is not uniquely determined for a given set of parameter values, it is not a straightforward problem to find the “true” minimum of the RSS. Consequently, even when the parameter space is scanned evenly, the precision is expected to be worse than the theoretically expected 2.5% threshold.

We found that the SA search outperforms the simple scanning, thanks to the SA algorithm’s ability to search low-RSS-value regions in the parameter space more heavily. On the whole, although the precision was not outstanding, our SA-based optimization method was still able to identify the RD network parameter values quantitatively, thus, it may be used as a valuable tool to analyze experimentally observed fluorescence fluctuations.

3.4. Perturbations to the Rho signaling network were detected by the RD system identification

Next, we have examined if our RD system identification method could detect perturbations applied to the biosignaling reaction network. All perturbations we applied to the simulation model were inhibitory: In the CA model, the Rho inactivation rate, k_{inact} was decreased by $\Delta k_{\text{inact}} = -0.099 \text{ s}^{-1}$ (see Table 3). Our SA search revealed a corresponding decrease of $\Delta k_{\text{inact}} = -0.087 \text{ s}^{-1}$. Similarly, in the CS mutant, the SA search revealed a decrease of 0.0392 s^{-1} in the Rho-membrane association rate, k_{on} , compared with the exact value of 0.0396 s^{-1} decrease. As seen in Fig. 5, our system identification method has located the altered RD systems in the 2D parameter space remarkably well, clearly elucidating the altered dynamics in the mutated Rho reaction models. Interestingly, in terms of determining the absolute values of k_{inact} and k_{on} , the corresponding errors were large. The cause of the low precision can be accounted as follows: The perturbations to the system were rate inhibitions by 100-fold in the both mutants. As a consequence, the reaction rates that were inhibited became vanishingly small, thus, the corresponding reactions hardly contribute to the observed spatio-temporal fluctuation patterns, leading to large relative uncertainty during parameter inversion. In some cases, one might consider setting these very small rates to zero in the RD network, if they are expected not to contribute much to the RD dynamics.

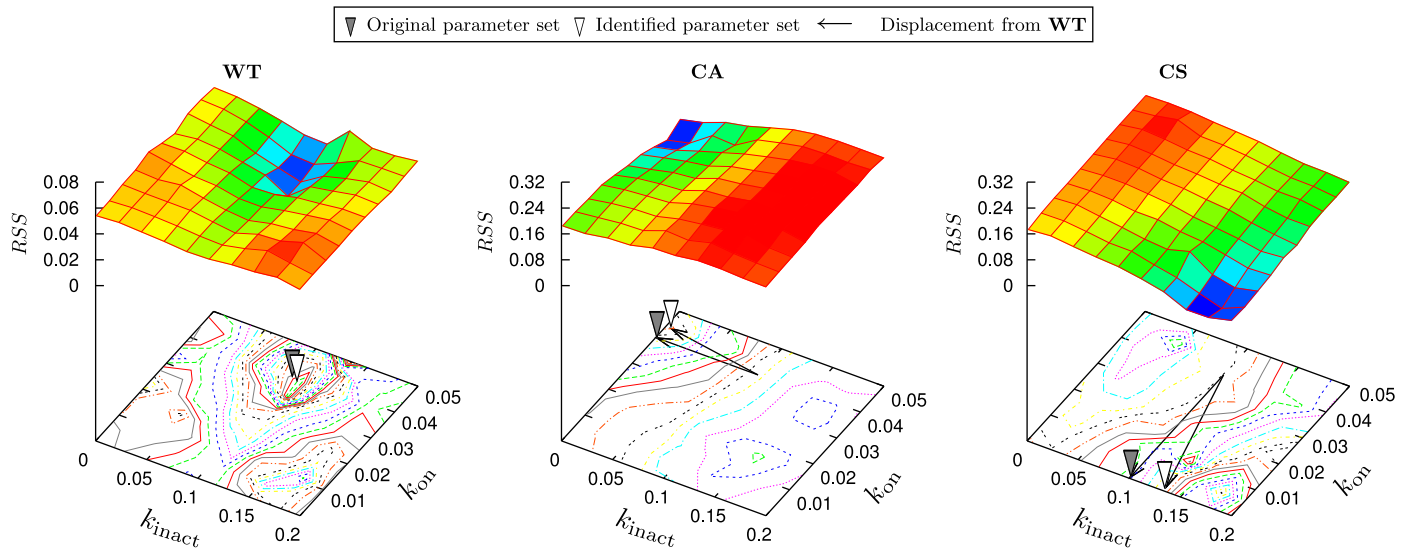


Fig. 5. The RSS landscapes in the two-dimensional parameter space. Each landscape was computed from the SA trajectory that has achieved the lowest RSS value among the 100 runs. The 1600 points in the two-dimensional parameter space were explored in a single run, and the landscape was generated by smoothing these 1600 points. The contour maps projected on the bottom plane is computed from the same data. The filled wedges on the contour maps point to the original model parameter values, and the open wedges point to the values found by the RD system identification. The arrows in CA and CS models show the displacements from the original WT parameter values.

Table 3
Reaction-network “mutations” are detected in the CA and CS models.

CA (RSS=0.00569)	Original	Identified	Error	Error-interval ratio ^a (%)
$\Delta k_{\text{inact}} \text{ (s}^{-1}\text{)}$	-0.099	-0.087	+0.012	+6.0
$\Delta k_{\text{on}} \text{ (s}^{-1}\text{)}$	± 0.000	+0.0035	+0.0035	+7.0
CS (RSS=0.00309)	Original	Identified	Error	Error-interval ratio ^a (%)
$\Delta k_{\text{inact}} \text{ (s}^{-1}\text{)}$	± 0.000	+0.033	+0.033	+17
$\Delta k_{\text{on}} \text{ (s}^{-1}\text{)}$	-0.03960	-0.03920	+0.00038	+0.8

^a The error-interval ratio values were calculated by the same formula used in Table 2.

Overall, our RD system identification method could successfully reverse-engineer the parameter values for simple Rho signaling networks. Despite concerns about absolute precision for vanishingly small rates, the RD system identification method can quantitatively characterize the relative rate changes between the three small GTPase signaling models. Therefore, the fluorescence fluctuation analysis of fluorescence microscopy data may serve as a powerful tool for differentiating among various candidate biosignaling RD models and obtaining a good guess for the model parameters.

3.5. Analysis of fluorescence microscopy data of Rho activation in living cells

The combination of fluorescence probes and video microscopy enables direct observation of biomolecular activities in living cells with a notably high spatial and temporal resolutions. Here we show that our STCF analysis can capture the characteristics of the spatio-temporal fluctuations of FRET signals of Rho (Fig. 6), which has been observed recently (Pertz et al., 2006). These particular data were recorded at a slow rate (1 frame/min), because the main purpose of this measurement was to observe the cell's morphological change and Rho activation pattern simultaneously. Thus, these experimental data are not directly comparable with our computational results, because the number fluctuations due to the reactions and diffusion are not captured at

this time scale. Still, our STCF analysis allows to distinctively characterize the spatio-temporal patterns of fluorescence signals from different sources.

We have computed the STCFs of fluorescence patterns from two different sites of the lamellipodial region of the cell (Fig. 6 A). In the Rho activity FRET biosensor, FRET-pair fluorescent proteins (CFP and YFP) are genetically fused into the Rho gene. When this gene product is in the activated form (GTP is bound to Rho moiety of the protein), the RBD (Rho-binding domain) that is fused to the N-terminus of this protein binds to the effector binding site of the Rho moiety, bringing CFP and YFP close enough to cause FRET (see Fig. 6 B). The FRET signal (the panel A right) reports the activation of Rho, while the YFP (left) shows the total amount of Rho biosensor at the site.

As shown in Fig. 6 E, the Rho activity in the living cell exhibits highly dynamic fluctuating patterns. Fig. 6 C shows the STCFs calculated from two regions of the cell (indicated in Fig. 6 A). The cause of the fluctuating patterns of FRET signals is unknown, to our knowledge. It is not likely that they are caused by the number fluctuations of Rho due to reactions and diffusion which we have discussed in this paper, since the recording time scale was 1 min. However, it may be possible that the Rho activity is controlled in a certain type of RD system where the dynamic pattern emerges at this timescale, known as dynamic Turing pattern formation (Loose et al., 2008). Another possibility is an existence of a dynamic heterogeneous structure in the medium that is involved in Rho activation, such as membrane rafts or a molecular complexes such

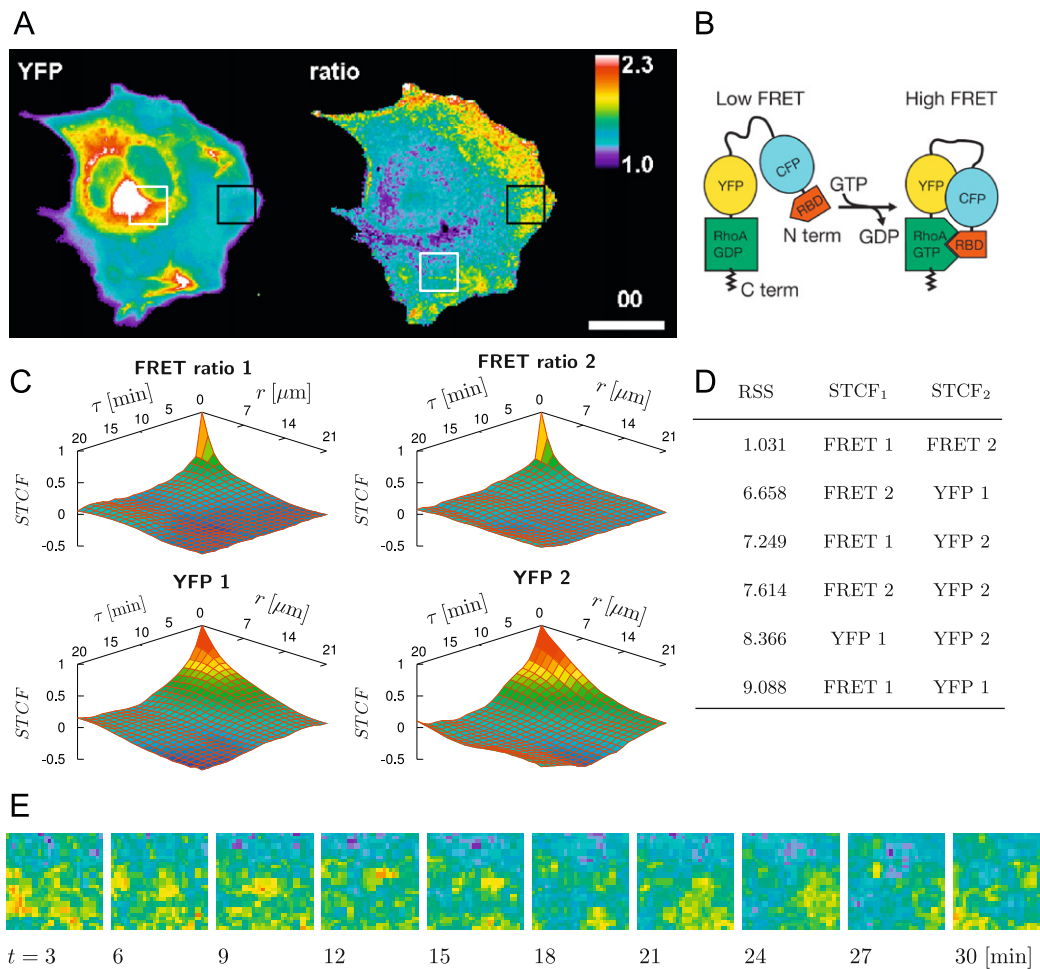


Fig. 6. Dynamic fluctuations of fluorescent signals from FRET-based biosensor-tagged Rho small GTPase in the living cell are shown. (Panels A, B and E are adapted from Pertz et al., 2006 with the authors' permission.) (A) Rho activation in a migrating mouse embryonic fibroblast cell. (B) The design of Rho activation biosensor. The image labeled YFP in the panel A is the color-coded fluorescence intensity of YFP, *ratio* is the ratio of the FRET signal intensity to the YFP fluorescence intensity. (C) STCFs of the FRET ratio ($H/(H+L)$, see text) calculated from the microscopy video data. The 30×30 pixel subsections of the video images are taken from two different regions of the cell (black box and white box in A, correspondingly labeled 1 and 2 in panels C and D). (D) RSS values for the STCFs in C. (E) Time-lapse image series of FRET video data from *ratio* 1 data. The scale bar is $30 \mu\text{m}$. (For interpretation of the references to color in this figure legend, the reader is referred to the web version of this article.)

as formation of signalosomes (Wei et al., 2008) or scaffolds (Pullikuth and Catling, 2007). Although this is beyond the scope of this paper, it may be interesting to perform a deterministic RD simulations to compare model predictions with experimental observations to elucidate the spatio-temporal RD patterns observed at this timescale.

The STCFs of the YFP fluorescence intensity obtained from the two different sites of the cell were dissimilar to each other ($RSS=8.366$), whereas the STCFs of the FRET signals are similar ($RSS=1.031$) (Fig. 6 C, D). The large difference in YFP spatio-temporal distribution patterns may be ascribed to the cell's movement during this video recording: The YFP fluorescence intensity indicates the amount of Rho-biosensor molecules at the position rather than the reaction–diffusion dynamics. Therefore, the YFP fluorescence intensity is proportional to the thickness of the cell, and the thickness of the cell may dynamically change as the cell moves.

Thus, the STCF analysis of experimentally observed Rho FRET biosensor images showed that the Rho activation exhibits a substantial spatial and temporal correlations at this timescale, and that the distribution dynamics of YFP signal, which indicates the total amount of Rho biosensor, apparently reflects the cell's movement. If the video data are recorded with a temporal resolution high enough to capture the number fluctuations due

to reactions and diffusion, the computational analysis developed in this study may provide further information about the dynamics and mechanism of this signaling molecule.

4. Conclusions

Aiming to elucidate intricate biosignaling reaction networks from video microscopy experiments, we have developed a method to analyze spatio-temporal fluorescence fluctuations that combines stochastic RD simulations, a STCF analysis, and a SA-based system identification technique. We have shown that the reaction dynamics and the diffusion of molecules in the RD systems are well represented in the STCFs computed from the corresponding spatio-temporal number fluctuations. The iterative SA optimization technique used in this study could successfully reverse-engineer the kinetic parameter values of the Rho RD system. Also, perturbations to the RD systems were well characterized using the same method.

The precision of our analysis method was only moderate, due to the lower resolution limits of CCD cameras compared to detectors used in FCS, and the compromised efficiency of SA optimization due to the inherent stochastic nature of the fluctuations. However, we have shown that, despite these

precision limits, analyzing fluorescence fluctuation in both the spatial and temporal dimensions can provide remarkably rich information about complex RD systems that cannot be reached otherwise. FCS may also be used for measuring diffusion coefficients or reaction rates, however, one needs to make simplifying theoretical assumptions to extrapolate the time-series data to the dynamics of spatio-temporal RD system, which severely restricts probing of more complex biological RD systems.

While the CCD camera time resolution sets the resolution limit of the STCF analysis, it is worth noting that correlation analysis intrinsically features a kind of band-pass filter that can help eliminate unwanted noise components from the signal to be analyzed. We discussed above that if an input signal has a characteristic correlation time less than the temporal resolution of the STCF, the STCF of such a signal becomes δ function-like. This, in turn, may be helpful in filtering out the thermal noise from the CCD camera. When weak signals are observed in video microscopy observes, the obtained video images are masked with CCD thermal noises. However, since this noise, originated from thermal motions of electrons, is much faster in time scale than the CCD camera temporal resolution, in the STCF analysis, this noise component is concentrated into a δ function-like spike at the origin, leaving the shape of STCF from the true signal intact. Thus, thanks to the time-scale difference in the fluorescence fluctuations and CCD thermal noise, the STCF easily separates these two components. For the similar reason, the STCF analysis would also work well at excluding static background noises, such as caused by an unevenness of the fluorescence excitation illumination source (this time the noise has a much slower characteristic time scale than the desired true signal).

In summary, the current analysis approach may be effectively applied to experimental observations with some advantages over the existing methods. Currently, a common way to measure diffusion coefficients *in vivo* is based on fluorescence recovery after photobleaching (FRAP). However, FRAP may perturb cell's biochemical systems crucially, as it needs to bleach fluorescently labeled molecules. The fluctuation-based analyses may serve as a much less invasive alternative to FRAP, as it does not require harsh photobleaching (this is not a problem in FCS), allowing repetitive observation of the same living cell sample for long periods of time. Also, our SA-based reverse-engineering technique can be extended to other applications with different timescales and length scales. For example, biological RD systems sometimes exhibit chemical oscillations, which exhibit distinctive spatio-temporal dynamic patterns (Loose et al., 2008). With an appropriate deterministic RD simulator, the SA-based analysis technique may serve as an effective analysis method for elucidating such RD systems.

Acknowledgements

We thank Dr. Klaus Hahn for stimulating discussions and kindly providing us with video microscopy data for Rho activation in a migrating mouse embryonic fibroblast cell. We would like to acknowledge financial support from the National Science Foundation under Grant CHE-715225 and CAREER Award CHE- 0846701. All calculations were carried out using the UNC Topsail super-computer.

References

Acar, M., Mettetal, J., van Oudenaarden, A., 2008. Stochastic switching as a survival strategy in fluctuating environments. *Nat. Genet.* 40 (4), 471–475, doi:10.1038/ng.110.

- Adams, S., Harootunian, A., Buechler, Y., Taylor, S., Tsien, R., 1991. Fluorescence ratio imaging of cyclic AMP in single cells. *Nature* 349 (6311), 694–697, doi:10.1038/349694a0.
- Artyomov, M.N., Das, J., Kardar, M., Chakraborty, A.K., 2007. Purely stochastic binary decisions in cell signaling models without underlying deterministic bistabilities. *Proc. Natl. Acad. Sci. USA* 104 (48), 18958–18963, doi:10.1073/pnas.0706110104.
- Bachir, A., Kolin, D., Heinze, K., Hebert, B., Wiseman, P., 2008. A guide to accurate measurement of diffusion using fluorescence correlation techniques with blinking quantum dot nanoparticle labels. *J. Chem. Phys.* 128 (22), 225105, doi:10.1063/1.2918273.
- Bakal, C., Linding, R., Llense, F., Heffern, E., Martin-Blanco, E., Pawson, T., Perrimon, N., 2008. Phosphorylation networks regulating JNK activity in diverse genetic backgrounds. *Science* 322 (5900), 453–456, doi:10.1126/science.1158739.
- Barrios-Rodiles, M., Brown, K., Ozdamar, B., Bose, R., Liu, Z., Donovan, R., Shinjo, F., Liu, Y., Dembowy, J., Taylor, I., Luga, V., Przulj, N., Robinson, M., Suzuki, H., Hayashizaki, Y., Jurisica, I., Wrana, J., 2005. High-throughput mapping of a dynamic signaling network in mammalian cells. *Science* 307 (5715), 1621–1625, doi:10.1126/science.1105776.
- Burkhardt, M., Schwille, P., 2006. Electron multiplying CCD based detection for spatially resolved fluorescence correlation spectroscopy. *Opt. Exp.* 14, 5013–5020.
- Bünemann, M., Frank, M., Lohse, M., 2003. G_i protein activation in intact cells involves subunit rearrangement rather than dissociation. *Proc. Natl. Acad. Sci. USA* 100 (26), 16077–16082, doi:10.1073/pnas.2536719100.
- Cai, L., Friedman, N., Xie, X., 2006. Stochastic protein expression in individual cells at the single molecule level. *Nature* 440 (7082), 358–362, doi:10.1038/nature04599.
- Chang, H., Hemberg, M., Barahona, M., Ingber, D., Huang, S., 2008. Transcriptome-wide noise controls lineage choice in mammalian progenitor cells. *Nature* 453 (7194), 544–547, doi:10.1038/nature06965.
- Chen, X., Xu, H., Yuan, P., Fang, F., Huss, M., Vega, V., Wong, E., Orlov, Y., Zhang, W., Jiang, J., Loh, Y., Yeo, H., Yeo, Z., Narang, V., Govindarajan, K., Leong, B., Shahab, A., Ruan, Y., Bourque, G., Sung, W., Clarke, N., Wei, C., Ng, H., 2008. Integration of external signaling pathways with the core transcriptional network in embryonic stem cells. *Cell* 133 (6), 1106–1117, doi:10.1016/j.cell.2008.04.043.
- Choi, P., Cai, L., Frieda, K., Xie, X., 2008. A stochastic single-molecule event triggers phenotype switching of a bacterial cell. *Science* 322 (5900), 442–446, doi:10.1126/science.1161427.
- Cox, C.D., McCollum, J.M., Allen, M.S., Dar, R.D., Simpson, M.L., 2008. Using noise to probe and characterize gene circuits. *Proc. Natl. Acad. Sci.* 105 (31), 10809–10814, doi:10.1073/pnas.0804829105 arXiv: <http://www.pnas.org/content/105/31/10809.full.pdf+html>, <http://www.pnas.org/content/105/31/10809.abstract>.
- Das, R., Kolomeisky, A., 2008. Spatial fluctuations affect the dynamics of motor proteins. *J. Phys. Chem. B* 112 (35), 11112–11121, doi:10.1021/jp800982b.
- Dickson, R., Cubitt, A., Tsien, R., Moerner, W., 1997. On/offblinking and switching behaviour of single molecules of green fluorescent protein. *Nature* 388 (6640), 355–358, doi:10.1038/41048.
- Dunlop, M.J., Cox III, R.S., Levine, J.H., Murray, R.M., Elowitz, M.B., 2008. Regulatory activity revealed by dynamic correlations in gene expression noise. *Nat. Genet.* 40 (12), 1493–1498, doi:10.1038/ng.281.
- Elson, E., Madge, D., 1974. Fluorescence correlation spectroscopy. I. Conceptual basis and theory. *Biopolymers* 13, 1–27.
- Erbán, R., Frewen, T., Wang, X., Elston, T., Coifman, R., Nadler, B., Kevrekidis, I., 2007. Variable-free exploration of stochastic models: a gene regulatory network example. *J. Chem. Phys.* 126 (15), 155103, doi:10.1063/1.2718529.
- Förster, T., 1959. Transfer mechanisms of electronic excitation. *Discuss. Faraday Soc.* 27, 717.
- Giepmans, B., Adams, S., Ellisman, M., Tsien, R., 2006. The fluorescent toolbox for assessing protein location and function. *Science* 312 (5771), 217–224, doi:10.1126/science.1124618.
- Gillespie, D.T., 1977. Exact stochastic simulation of coupled chemical reactions. *J. Phys. Chem.* 81 (25), 2340–2361, doi:10.1021/j100540a008.
- Harada, T., Sasa, S., 2007. Fluctuations, responses and energetics of molecular motors. *Math. Biosci.* 207 (2), 365–386, doi:10.1016/j.mbs.2006.11.003.
- Hebert, B., Costantino, S., Wiseman, P., 2005. Spatiotemporal image correlation spectroscopy (STICS) theory, verification, and application to protein velocity mapping in living CHO cells. *Biophys. J.* 88 (5), 3601–3614, doi:10.1529/biophysj.104.054874.
- Hegener, O., Prenner, L., Runkel, F., Baader, S., Kappler, J., Häberlein, H., 2004. Dynamics of β_2 -adrenergic receptor-ligand complexes on living cells. *Biochemistry* 43 (20), 6190–6199, doi:10.1021/bi035928t.
- Inoué, S., Spring, K.R., 1997. *Video Microscopy: The Fundamentals*. Springer, New York.
- Isaacson, S., 2008. Relationship between the reaction-diffusion master equation and particle tracking models. *J. Phys. A Math. Theor.* 41 (6), 65003.
- Jaffe, A., Hall, A., 2005. Rho GTPases: biochemistry and biology. *Annu. Rev. Cell Dev. Biol.* 21, 247–269, doi:10.1146/annurev.cellbio.21.020604.150721.
- Janes, K., Albeck, J., Gaudet, S., Sorger, P., Lauffenburger, D., Yaffe, M., 2005. A systems model of signaling identifies a molecular basis set for cytokine-induced apoptosis. *Science* 310 (5754), 1646–1653, doi:10.1126/science.1116598.
- Janetopoulos, C., Jin, T., Devreotes, P., 2001. Receptor-mediated activation of heterotrimeric G-proteins in living cells. *Science* 291 (5512), 2408–2411, doi:10.1126/science.1055835.

- Kaern, M., Elston, T., Blake, W., Collins, J., 2005. Stochasticity in gene expression: from theories to phenotypes. *Nat. Rev. Genet.* 6 (6), 451–464, doi:10.1038/nrg1615.
- Kirkpatrick, S., Gelatt, C., Vecchi, M., 1983. Optimization by simulated annealing. *Science* 220 (4598), 671–680, doi:10.1126/science.220.4598.671.
- Kojima, H., Muto, E., Higuchi, H., Yanagida, T., 1997. Mechanics of single kinesin molecules measured by optical trapping nanometry. *Biophys. J.* 73 (4), 2012–2022, doi:10.1016/S0006-3495(97)78231-6.
- Kolin, D., Wiseman, P., 2007. Advances in image correlation spectroscopy: measuring number densities, aggregation states, and dynamics of fluorescently labeled macromolecules in cells. *Cell Biochem. Biophys.* 49 (3), 141–164, doi:10.1007/s12013-007-9000-5.
- Kolin, D., Ronis, D., Wiseman, P., 2006. k-Space image correlation spectroscopy: a method for accurate transport measurements independent of fluorophore photophysics. *Biophys. J.* 91 (8), 3061–3075, doi:10.1529/biophysj.106.082768.
- Kraynov, V., Chamberlain, C., Bokoch, G., Schwartz, M., Slabaugh, S., Hahn, K., 2000. Localized Rac activation dynamics visualized in living cells. *Science* 290 (5490), 333–337.
- Lan, Y., Papoian, G.A., 2006a. The interplay between discrete noise and nonlinear chemical kinetics in a signal amplification cascade. *J. Chem. Phys.* 125 (15), 154901, doi:10.1063/1.2358342.
- Lan, Y., Papoian, G.A., 2007a. Stochastic resonant signaling in enzyme cascades. *Phys. Rev. Lett.* 98 (22), 228301.
- Lan, Y., Papoian, G.A., 2007b. Evolution of complex probability distributions in enzyme cascades. *J. Theor. Biol.* 248 (3), 537–545, doi:10.1016/j.jtbi.2007.06.008.
- Lan, Y., Papoian, G.A., 2008. The stochastic dynamics of filopodial growth. *Biophys. J.* 94 (10), 3839–3852 <http://dx.doi.org/8>.
- Lan, Y., Wolynes, P.G., Papoian, G.A., 2006. A variational approach to the stochastic aspects of cellular signal transduction. *J. Chem. Phys.* 125 (12), 124106, doi:10.1063/1.2353835.
- Locasale, J.W., Shaw, A.S., Chakraborty, A.K., 2007. Scaffold proteins confer diverse regulatory properties to protein kinase cascades. *Proc. Natl. Acad. Sci. USA* 104 (33), 13307–13312, doi:10.1073/pnas.0706311104.
- Loose, M., Fischer-Friedrich, E., Ries, J., Kruse, K., Schwill, P., 2008. Spatial regulators for bacterial cell division self-organize into surface waves in vitro. *Science* 320 (5877), 789–792, doi:10.1126/science.1154413.
- Lu, H., Xun, L., Xie, X., 1998. Single-molecule enzymatic dynamics. *Science* 282 (5395), 1877–1882.
- Lu, S., Ouyang, M., Seong, J., Zhang, J., Chien, S., Wang, Y., 2008. The spatiotemporal pattern of Src activation at lipid rafts revealed by diffusion-corrected FRET imaging. *PLoS Comput. Biol.* 4 (7), e1000127, doi:10.1371/journal.pcbi.1000127.
- Lu, T., Shen, T., Bennett, M., Wolynes, P., Hasty, J., 2007. Phenotypic variability of growing cellular populations. *Proc. Natl. Acad. Sci. USA* 104 (48), 18982–18987, doi:10.1073/pnas.0706115104.
- Mattis, D.C., Glasser, M.L., 1998. The uses of quantum field theory in diffusion-limited reactions. *Rev. Mod. Phys.* 70 (3), 979, doi:10.1103/RevModPhys.70.979.
- Mettetal, J., Muzzey, D., Pedraza, J., Ozbudak, E., van Oudenaarden, A., 2006. Predicting stochastic gene expression dynamics in single cells. *Proc. Natl. Acad. Sci. USA* 103 (19), 7304–7309, doi:10.1073/pnas.0509874103.
- Miyawaki, A., Llopis, J., Heim, R., McCaffery, J., Adams, J., Ikura, M., Tsien, R., 1997. Fluorescent indicators for Ca²⁺ based on green fluorescent proteins and calmodulin. *Nature* 388 (6645), 882–887, doi:10.1038/42264.
- Mochizuki, N., Yamashita, S., Kurokawa, K., Ohba, Y., Nagai, T., Miyawaki, A., Matsuda, M., 2001. Spatio-temporal images of growth-factor-induced activation of Ras and Rap1. *Nature* 411 (6841), 1065–1068, doi:10.1038/35082594.
- Monine, M., Haugh, J., 2005. Reactions on cell membranes: comparison of continuum theory and Brownian dynamics simulations. *J. Chem. Phys.* 123, 074908.
- Nalbant, P., Hodgson, L., Kraynov, V., Touthkine, A., Hahn, K., 2004. Activation of endogenous Cdc42 visualized in living cells. *Science* 305 (5690), 1615–1619.
- Parent, C., Blacklock, B., Froehlich, W., Murphy, D., Devreotes, P., 1998. G protein signaling events are activated at the leading edge of chemotactic cells. *Cell* 95 (1), 81–91.
- Pertz, O., Hodgson, L., Klemke, R., Hahn, K., 2006. Spatiotemporal dynamics of RhoA activity in migrating cells. *Nature* 440 (7087), 1069–1072.
- Petráček, Z., Schwill, P., 2008. Fluctuations as a source of information in fluorescence microscopy. *J. R. Soc. Interface* 6, S15–S25, doi:10.1098/rsif.2008.0200.focus.
- Petty, H., 2007. Fluorescence microscopy: established and emerging methods, experimental strategies, and applications in immunology. *Microsc. Res. Tech.* 70 (8), 687–709, doi:10.1002/jemt.20455.
- Pullikuth, A., Catling, A., 2007. Scaffold mediated regulation of MAPK signaling and cytoskeletal dynamics: a perspective. *Cell. Signal.* 19 (8), 1621–1632, doi:10.1016/j.cellsig.2007.04.012.
- Sakamoto, T., Webb, M., Forgacs, E., White, H., Sellers, J., 2008. Direct observation of the mechanochemical coupling in myosin Va during processive movement. *Nature* 455 (7209), 128–132, doi:10.1038/nature07188.
- Sasaki, K., Sato, M., Umezawa, Y., 2003. Fluorescent indicators for Akt/protein kinase B and dynamics of Akt activity visualized in living cells. *J. Biol. Chem.* 278 (33), 30945–30951, doi:10.1074/jbc.M212167200.
- Starr, T., Thompson, N., 2001. Total internal reflection with fluorescence correlation spectroscopy: combined surface reaction and solution diffusion. *Biophys. J.* 80 (3), 1575–1584.
- Svoboda, K., Mitra, P., Block, S., 1994. Fluctuation analysis of motor protein movement and single enzyme kinetics. *Proc. Natl. Acad. Sci. USA* 91 (25), 11782–11786.
- Violin, J., Zhang, J., Tsien, R., Newton, A., 2003. A genetically encoded fluorescent reporter reveals oscillatory phosphorylation by protein kinase C. *J. Cell Biol.* 161 (5), 899–909, doi:10.1083/jcb.200302125.
- Walczak, A., Sasai, M., Wolynes, P., 2005. Self-consistent proteomic field theory of stochastic gene switches. *Biophys. J.* 88 (2), 828–850, doi:10.1529/biophysj.104.050666.
- Warmflash, A., Dinner, A.R., 2008. Signatures of combinatorial regulation in intrinsic biological noise. *Proc. Natl. Acad. Sci.* 105 (45), 17262–17267, doi:10.1073/pnas.0809314105 arXiv: <http://www.pnas.org/content/105/45/17262.full.pdf+html>, <http://www.pnas.org/content/105/45/17262.abstract>.
- Wawrezinieck, L., Rigneault, H., Marguet, D., Lenne, P., 2005. Fluorescence correlation spectroscopy diffusion laws to probe the submicron cell membrane organization. *Biophys. J.* 89 (6), 4029–4042, doi:10.1529/biophysj.105.067959.
- Wei, N., Serino, G., Deng, X., 2008. The COP9 signalosome: more than a protease. *Trends Biochem. Sci.* 33 (12), 592–600, doi:10.1016/j.tibs.2008.09.004.
- Yu, H., Braun, P., Yildirim, M., Lemmens, I., Venkatesan, K., Sahalie, J., Hirozane-Kishikawa, T., Gebreab, F., Li, N., Simonis, N., Hao, T., Rual, J., Dricot, A., Vazquez, A., Murray, R., Simon, C., Tardivo, L., Tam, S., Svrikapa, N., Fan, C., de Smet, A., Motyl, A., Hudson, M., Park, J., Xin, X., Cusick, M., Moore, T., Boone, C., Snyder, M., Roth, F., Barabasi, A., Tavernier, J., Hill, D., Vidal, M., 2008. High-quality binary protein interaction map of the yeast interactome network. *Science* 322 (5898), 104–110, doi:10.1126/science.1158684.
- Zhang, J., Ma, Y., Taylor, S., Tsien, R., 2001. Genetically encoded reporters of protein kinase A activity reveal impact of substrate tethering. *Proc. Natl. Acad. Sci. USA* 98 (26), 14997–15002, doi:10.1073/pnas.211566798.
- Zhang, Z., Rajagopalan, P., Selzer, T., Benkovic, S., Hammes, G., 2004. Single-molecule and transient kinetics investigation of the interaction of dihydrofolate reductase with NADPH and dihydrofolate. *Proc. Natl. Acad. Sci. USA* 101 (9), 2764–2769, doi:10.1073/pnas.0400091101.
- Zhuravlev, P.I., Papoian, G.A., 2009. Molecular noise of capping protein binding induces macroscopic instability in filopodial dynamics. *Proc. Natl. Acad. Sci. USA* 106, 1570–1575, doi:10.1073/pnas.0812746106 arXiv: <http://www.pnas.org/content/early/2009/06/24/0812746106.full.pdf+html>.
- van Kampen, N., 1992. *Stochastic Processes in Physics and Chemistry*. Elsevier Science, Amsterdam.
- van der Wal, J., Habets, R., Vrnai, P., Balla, T., Jalink, K., 2001. Monitoring agonist-induced phospholipase C activation in live cells by fluorescence resonance energy transfer. *J. Biol. Chem.* 276 (18), 15337–15444, doi:10.1074/jbc.M007194200.